Running beyond the bio-inspired regime

Duncan W. Haldane, and Ronald S. Fearing

***Abstract*— The X2-VelociRoACH is a 54 gram experimental legged robot which was developed to test hypotheses about running with unnaturally high stride frequencies. It is capable of running at stride frequencies up to 45 Hz, and velocities up to 4.9 m/s, making it the fastest legged robot relative to size. The top speed of the robot was limited by structural failure. We present new methods and materials to make more robust folded robotic structures. High-frequency running experiments with the robot shows that the power required to cycle its running appendages increase cubically with the stride rate. Our findings show that although it is possible to further increase the maximum velocity of a legged robot with the simple strategy of increasing stride frequency, considerations must be made for the energetic demands of high stride rates.**

I. Introduction

As we seek to build ever improving legged robots, it is a useful exercise to investigate the efficacy of locomotion strategies in their respective limits. By having knowledge of system behavior at extremes we can more effectively guide the development of future platforms. In this work we explore increasing the maximum attainable speed of a legged robotic platform by pushing its stride frequency to an extreme value.

Animals have a well-defined approach to running at high velocities. Fig. 2 is a plot of stride frequency vs non-dimensional speed for the VelociRoACH [16] and *P. americana*, the American cockroach. Non-dimensional speed is defined as the Froude number, $F = \frac{v}{\sqrt{gl}}$, where v is running speed, g is the gravitational constant, and l is leg length. The running dynamics of *P. americana* were used to establish targets for the VelociRoACH, and previous research has shown that the two systems are dynamically similar [15][16]. The difference between the trends in this figure signify a fundamental difference between running animals and running robots. The knee in the cockroach data in Fig. 2 indicates the stride frequency limit, the point at which the musculo-skeletal locomotory system of the cockroach can drive the legs no faster. This limit exists for multiple species [13], such as ghost crabs [7], dogs [17], and cheetahs [21]. The common trend across these species is that the animal will run near its stride frequency limit, and increase velocity by increasing stride length. This is as opposed to the trend in the VelociRoACH data wherein the speed increases linearly with stride frequency. The VelociRoACH's leg kinematics are not easily changed because they are rigidly defined by kinematic structures which couple the output of two separate motors to drive a total of six legs [16].

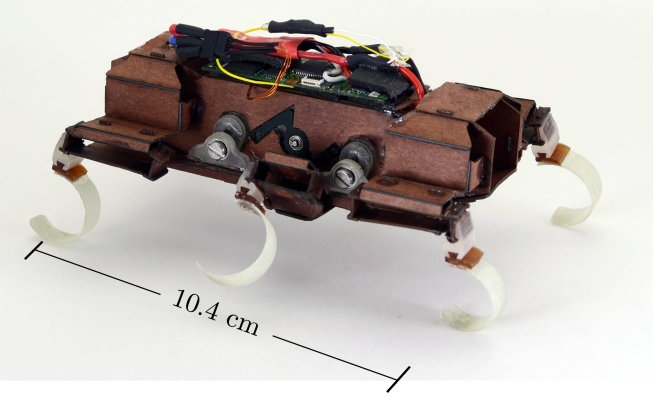

Fig. 1: The X2-VelociRoACH, built to test hypotheses about high-frequency running

Limitations on stride kinematics are common across many dynamic running robots. iSprawl[22] had only a single drive actuator, with two servos to adjust the angle of each middle leg in the saggital plane. The RHex robot has a total of six motors, each controlling the angle of one of its six legs. Kinematic adaptations which would increase the stride length of these robots are possible, but they incur a cost in complexity either in hardware, control, or both. The other option to increase speed is to simply increase the stride frequency of the system without altering the kinematics. This is the strategy adopted by VelociRoACH. As shown in Fig. 2, the stride frequency was simply increased until the robot reached the same non-dimensional velocity as the cockroach. This stride frequency is unnaturally high for a running system of VelociRoACH's mass.

The stride frequency limit of an animal can generally be predicted by its body mass [13]. This result is an effect of underlying principles of dynamic similarity across a wide array of terrestrial animals [1][8]. These principles establish underlying locomotory dynamics which are invariant across size scales. Given several animal examples, gait characteristics such as velocity, or stride frequency can be determined for a robotic system using dynamic similarity scaling [16][2][11]. The stride frequency limit for several animals is plotted against their body mass in Fig. 3. Dynamic scaling expects that the stride frequency of smaller animals

This material is based upon work supported by the National Science Foundation under IGERT Grant No. DGE-0903711, and Grant No. CNS-0931463, and the United States Army Research Laboratory under the Micro Autonomous Science and Technology Collaborative Technology Alliance.

D.W. Haldane is with the Department of Mechanical Engineering, University of California, Berkeley, CA 94720 USA, *dhaldane@berkeley.edu*

R.S. Fearing is with the Department of Electrical Engineering and Computer Sciences, University of California, Berkeley, CA 94720 USA, *ronf@eecs.berkeley.edu*

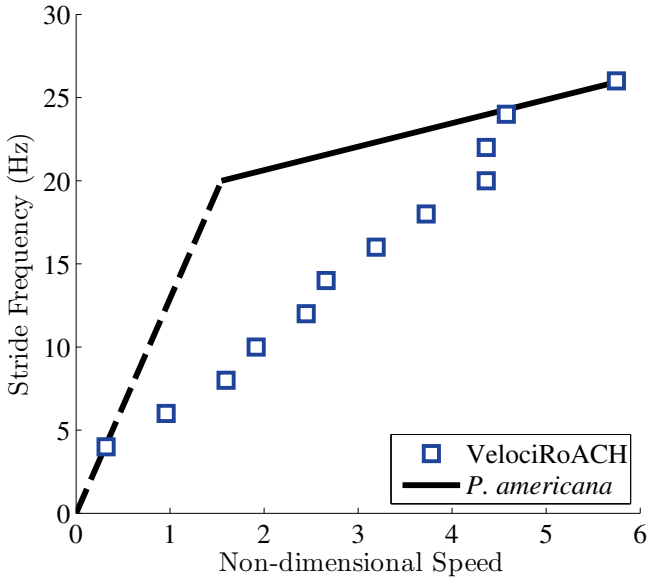

Fig. 2: Stride frequency vs non-dimensional speed for the American cockroach (trend-line extracted from Full & Tu [14]) and VelociRoACH [16]. The non-dimensional speed is equivalent to the Froude number (defined in text). The dotted line indicates walking behaviors, the solid line indicates running. The VelociRoACH has a running gait (defined by the presence of an aerial phase) above 8 Hz.

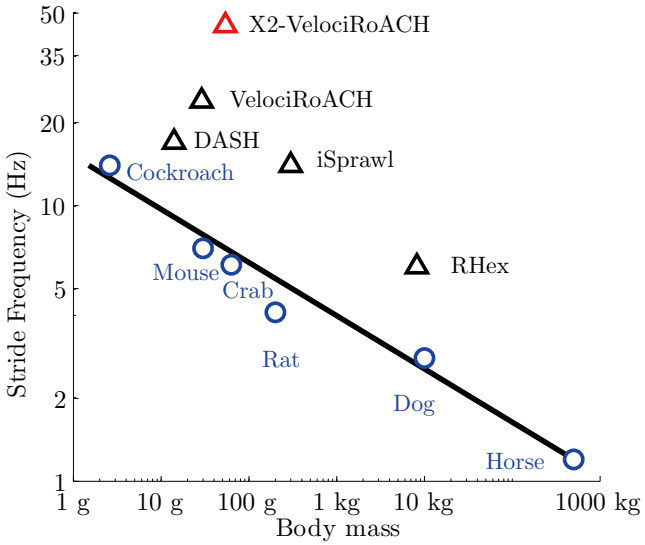

Fig. 3: Stride frequency vs body mass for a range of running animals and robots. Animal data from Full [13]. The X2-VelociRoACH presented in this work has the highest stride frequency of any extant running robot.

will be higher than that of larger animals[1]. Also shown in Fig. 3 are the masses and stride frequency limits of several running robotic platforms. All of these platforms are capable of a higher stride frequency than an animal of the same mass would be expected to use. Engineered systems such as these legged robots are not subject to the same physiological constraints as their animal counterparts, so it is reasonable that these robots have used an increased stride frequency to increase the span of velocities that they are able to achieve. An area that has not been fully explored is what happens when the stride frequency of a robot is pushed even higher. The trade-offs that occur in this operating regime have not been assessed. Addressing these questions will inform the design of future running robots.

In this work we present the design of the experimental robotic platform, X2-VelociRoACH, which has been created to test what happens to legged locomotion in the frequency limit. The design and fabrication of the platform is shown in Section II. Results from high-frequency running experiments are given in Section III. The principles of locomotion with unnaturally-high stride frequencies are given in Section IV.

II. Methods

A. Design and Construction of the X2-VelociRoACH

The X2-VelociRoACH was built to test hypotheses about the characteristics of running at unnaturally high stride frequencies. We based the design on the extant running robot, VelociRoACH. VelociRoACH was made using the Smart Composite Microstructures (SCM) process which creates linkages by combining rigid and flexible materials using planar processes [20]. It has been used to create several milliscale [6][26][19][16] and microscale [5][18] legged robots. Linkages made with SCM have been used reduce the requisite number of actuators for legged robots which allows for the use of larger, more power dense actuators. The geometric parameters of the SCM kinematic linkages which couple motor rotation to leg motion were maintained between VelociRoACH and the X2-VelociRoACH, so both robots have the same stride kinematics. This allows for a point of direct comparison the prior art. A number of challenges had to be overcome to make the X2-VelociRoACH a reality. Firstly, the power density of the platform had to increase to make more power available for cycling the legs more quickly. Secondly, the coupling between the motor and the SCM linkages had to be rigidified. The robustness of the SCM components had to be increased to cope with the loads exerted on the robot by the legs.

1) Power transmission: The original VelociRoACH used two coreless brushed DC motors to drive its legs, one for either side of the robot [16]. To increase the power density of the new platform we replaced these motors with a single out-runner brushless motor the *Air King AX-1306*. This motor has a listed voltage constant of $K_v = 2200\frac{\text{rpm}}{\text{V}}$, phase winding resistance of 0.88Ω, and current limit of 6A. We statically measured the torque constant to be $5.5\frac{\text{mNm}}{\text{A}}$, which indicates a somewhat lower K_v of $1720\frac{\text{rpm}}{\text{V}}$. The estimated maximum rotational frequency (for a 7.4V battery, after gearing) is then 85 Hz; the maximum torque produced would be 81 mNm. This motor weighs nine grams and has a peak output

[1]The stride frequency scales with $\sim \alpha_M^{-0.17}$ where α_M is the ratio of masses of the two systems being compared.

power of 6.5 W after gearing. X2-VelociRoACH therefore has significantly more power than VelociRoACH, whose two motors have a combined peak power output of 1.3 W.

The hobby-grade motor used in the X2-VelociRoACH is far less expensive than high-quality brushless motors like the *Faulhaber 0602*[2] and is more power-dense (but less efficient). The out-runner form factor of the motor allows for a large gap radius, reducing the requisite gear ratio. In conjunction with the smart composite microstructures process, the low cost allows us to stay within the paradigm of ultra-low cost microrobots, to which VelociRoACH belongs. For all their advantages hobby-grade motors of this type have a major downside for the purposes of legged robotics: they have no Hall effect sensors to specify commutation of the motor. Lacking a specialized micro-scale brushless motor controller, we have employed a hobby-grade sensorless electronic speed controller (ESC) (*Hobbyking 6A ESC*). Controllers of this type measure the back-EMF generated by the spinning motor to control commutation which has several implications: they have a high minimum speed, and they do not cope well with varying loads. This second point is critical, the inability these controllers to cope with the slightly varying loads from a flapping mechanism in a MAV [25] caused complications; the impact loads generated by legged locomotion cause greater ones (see Section III).

The X2-VelociRoACH's transmission is shown in Fig 4. The brushless motor drives two cranks through a single 2.48:1 reduction, which puts the maximum power point of the motor at a stride frequency of 50 Hz. This dual drive constrains the drive layer of the robot to be parallel, replacing the parallel four-bar mechanism that served the same function in VelociRoACH [16]. Previous SCM robots [16][19][26] used a simple pin-bushing connection to couple crank rotation to the SCM layer. This strategy did not properly constrain the drive plate at high velocities so we employed bearings mounted in 3D printed plastic, which were connected to the crank with a shoulder bolt (as can be seen in Fig. 1). We sought to enable the rapid fabrication of this robot, thus the majority of the transmission was 3D printed, including the gears. The 3D printed plastic material was not strong enough to use as a drive shaft so hollow shafts were printed, which were internally reinforced with carbon-fiber tubing.

This transmission physically constrains the gait of the X2-VelociRoACH to alternating tripod, as shown in Fig. 4B, meaning it cannot use differential steering like previous robots [16][26]. However we have shown that simple differential steering is not desirable for repeatable dynamic running [10], and steering can be more readily accomplished using a multi-functional inertial [24], or aerodynamic [23] appendage. Steering is unnecessary for the experimental goals for the X2-VelociRoACH; it can be added later to enable field operation.

2) Damage mitigation: It has been proposed that animals running at high stride frequencies incur higher peak forces

[2]Which has been used in other small scale robots, e.g. [9]

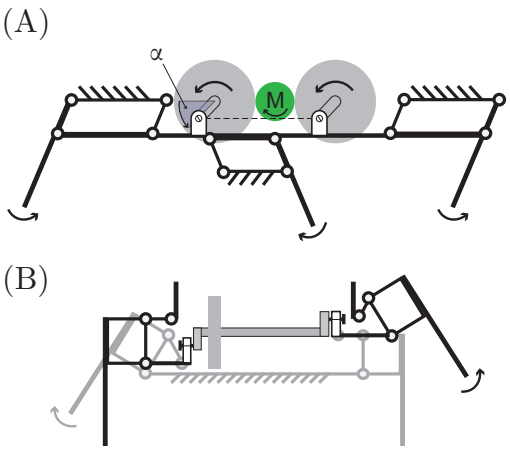

Fig. 4: A conceptual kinematic drawing of the X2-VelociRoACH's drive mechanism. (A) A side view of the mechanism. The motor (shown in green) drives two parallel crankshafts through two gears (shown in gray). (B) A front view of the mechanism showing how the driven cranks are offset by 180°, thereby constraining the gait to alternating tripod. The crank angle α is also shown on the figure.

[21]. This is certainly the case with the X2-VelociRoACH. Materials which have been previously used to create SCM millirobots are unable to withstand the high loads that occur in high frequency running. We observed that these loads are proportional to the inertia of the running appendages, so fiberglass legs were used. These legs were made with six layers of alternating $\pm 45°$ and $0°/90°$ S grade fiberglass in a wet-layup epoxy process. The fiberglass legs had 30% less inertia than the rubber legs used by VelociRoACH [16].

In the past, 25 μm polyethylene terephthalate (PET) film has been used for the flexure layer of several robots [16][19][26]. A X2-VelociRoACH made with PET was tested to destruction to determine the achievable stride frequency limit. While running in air, the inertial forces from the recirculating limbs were enough to destroy the flexures before the stride frequency reached 45 Hz. On the ground, one three second run at 32 Hz was enough to tear flexures. Tendons made of Kevlar filament placed across flexures were able to extend the running life by a small amount, but these failed eventually as well. We experimented with a composite of tough Spectra fibers sandwiched between two sheets of polyester film (*Cuben Fabric*) as a flexure layer. This material is similar in dimension and bonding chemistry to the PET film, and greatly extended the running life of the robot. However, flexures made with this material still failed after a few trials of high frequency running, as shown in Fig. 5a. We therefore decided to use rip-stop nylon (*1.9 oz Uncoated rip-stop nylon.* From *ripstopbytheroll.com*) as our flexure layer[3]. Flexures made with rip-stop nylon did not fail in any of our experiments. Instead, the rigid component of

[3] This material is now used in the flexure layer of the commercialized version of the DASH robot

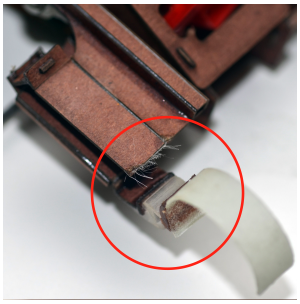

(a) A failed Cuben fabric flexure. Failure of this material was typified by fiber pullout.

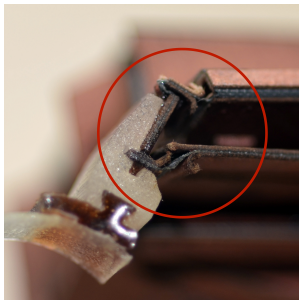

(b) The rigid material failing by peeling at a hip flexure.

Fig. 5: Failure modes of SCM mechanisms after high frequency running

the SCM composite began to fail at the highest achievable stride frequencies, as shown in Fig. 5b. This material failure is the limit for the top speed of the robot.

Despite these material limits, the X2-VelociRoACH was able to run on the ground at stride frequencies up to 45 Hz without incurring significant damage. More dynamic performance from this robot is achievable if new materials and processes that further increase the durability of SCM robots are developed.

B. Control electronics

The X2-VelociRoACH is driven by the imageProc 2.5[4] [3] robot control board. Motor current measurements are unavailable from the sensorless speed controller, so a low-side shunt resistor was used to measure current consumption for the entire robot. We estimated the motor power by offsetting the total power consumption by the levels recorded while the motor is powered down. A Hall-effect based encoder was placed on the brushless motor output to determine the position of the legs. The imageProc collects telemetry data including current measurements, battery voltage level, 6-axis inertial measurements, and motor position at 1000 Hz. The integrated 802.15.4 radio interface was used for communication and external control[5]. A 7.4V, 180mAh battery powered the robot, lasting for approximately twenty minutes before needing recharging.

C. Experiments

A number of experiments were conducted to determine the characteristics of high-frequency running. The X2-VelociRoACH was run without the legs touching the ground to establish the cost of recirculating the legs in the absence of any interaction with the ground. During these experiments, the robot was held firmly by hand. Another set of off-the-ground experiments were run with the robot's legs removed to determine the contribution of appendage inertia to the overall cost. Running experiments across a wide range of speeds were conducted on level closed-pile carpet. Motion data was collected from the robot by recording high-speed video at 600 frames per second, and digitizing visual markers with *Pro-Analyst* motion analysis software.

To facilitate data collection, all experiments were run with the same aerodynamic stabilizer developed for VelociRoACH [16]. All experiments were run on the same robot, with on-ground running first, appendages in the air second, and without appendages in the air last. For each experiment, a range of open-loop throttle commands was sent to the sensorless speed controller to explore the span of achievable performance.

[4]Embedded board: https://github.com/biomimetics/imageproc_pcb
[5]Embedded code: https://github.com/dhaldane/roach

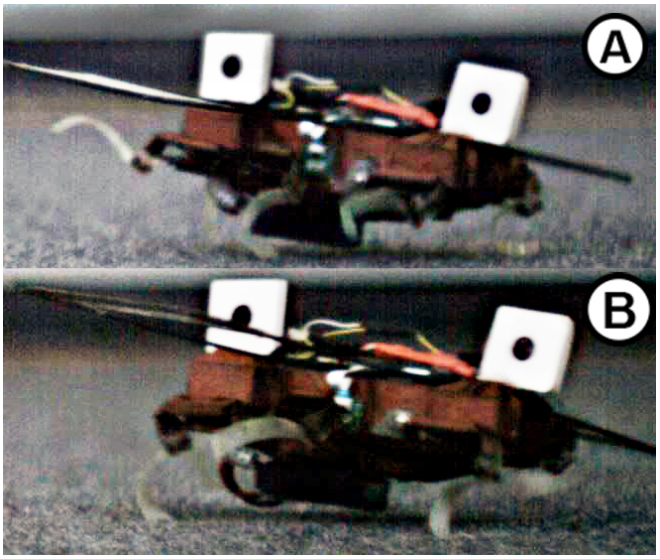

Fig. 6: Stills from a high-speed video (583 fps) of the X2-VelociRoACH running at 45 Hz.

III. Results

Fig. 6 shows several stills from a high-speed video of the robot running with a stride frequency of 45 Hz. These stills demonstrate behaviors typical to high frequency running. Fig. 6A shows hyper-extension of the flexible 'C' legs. High inertial forces occuring during high frequency running tend to stretch out the robot's appendages. There is also a significant increase in the robot's range of leg angles; inertial forces acting on the semi-compliant SCM mechanisms cause increases in both abduction and adduction angle. At high velocities the touchdown angle of the leg approaches the vertical, as shown in Fig. 6B. It should be noted that the battery of the X2-VelociRoACH is mounted on the bottom of the platform. It is very close to the ground, but never made contact in any of the experiments.

Fig. 7 shows the fore-aft acceleration of the X2-VelociRoACH over approximately 70 strides during steady state running at 45 Hz. This figure demonstrates the strong periodicity of high-frequency running gaits. Well defined regions of positive and negative acceleration (as have been well documented in low-frequency running) can also be seen.

Fig. 8a shows the speed of the X2-VelociRoACH as a function of stride frequency. The robot was unable to run at stride frequencies below 35 Hz due high impact loads interfering with the brushless ESC. Gaits in this lower frequency

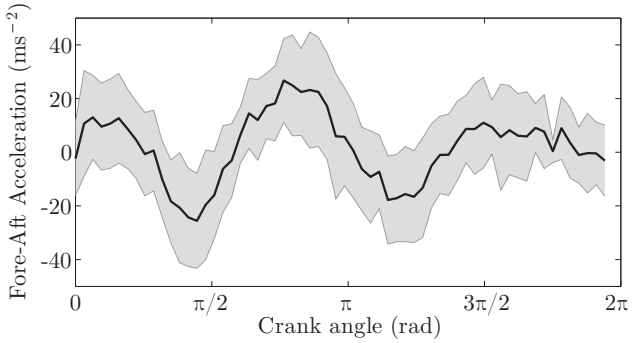

Fig. 7: Fore-aft accelerations of the X2-VelociRoACH running at 45 Hz as a function of the crank angle. Approximately 70 strides were averaged, the shaded region is one standard deviation.

region were typified by repeated motor stalls followed by $\sim$ 500 ms of rapid leg motion as the ESC attempted to generate a measurable back-EMF (electro-motive force) from the motor. This phenomena caused large perturbations in height and pitch angle as the robot attempted to proceed forward.

Above 35 Hz, in the regime of stable running, the forward velocity increased linearly with stride frequency to a maximum of 4.9 m/s, without significant changes in slope. Also shown on the graph is a kinematic limit on the velocity of the robot. The peak leg tip velocity occurs at mid-stance (as described in previous works [10]). If the robot were on the boundary of the kinematic limit, it would be moving at this top speed over the entire stride. Fig. 8b shows the average stride length of the robot as a function of stride frequency. The increasing trend in this graph shows that the robot travels a greater distance per stride at higher frequencies. This may be caused by an increase in the effective leg length caused by the previously discussed inertial forces. Alternatively, the robot could be generating impulses when the legs collide with the ground at high speeds. Because the leg touches down near the vertical these impulses would be propulsive, allowing the robot to generate additional thrust.

To estimate the effects of inertial loads during high-frequency locomotion we created a full simulation of the X2-VelociRoACH kinematic mechanism in Solidworks. Shown in Fig. 9a, this model has one degree of freedom and predicts the motor loading caused by inertial effects of the mechanism and appendages. The simulated motor drove the mechanism at a constant stride frequency, and Solidworks Motion was used to calculate the power required to produce the motion. Data from three of these simulations are presented in Fig. 9b. The peak power required increases cubically with the stride frequency, as would be expected for an inertial load forced to track a sinusoidal position input. To validate the Solidworks simulation, data from the robot running in air at 40 Hz are presented in Fig. 9c. This plot shows the crank angle with the cyclic trend removed, as a function of time, over one stride period. The sensorless speed controller drives the motor with an open-loop duty cycle, so we would expect

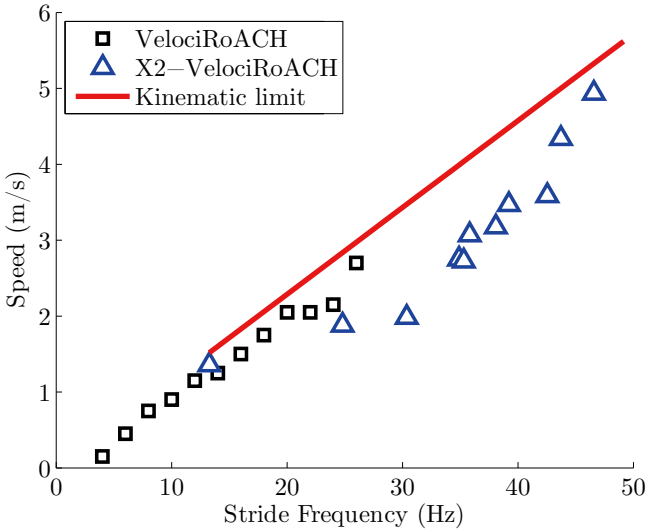

(a) Speed as a function of stride frequency for the X2-VelociRoACH, and VelociRoACH [16]. Also shown is a kinematic upper bound on the stride frequency.

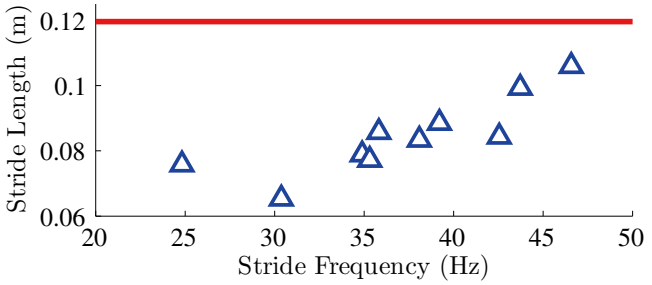

(b) Distance traveled over a single stride (one full crank rotation), as a function of stride frequency. The red line is the distance a robot with wheels of the same radius as the nominal leg length would travel.

Fig. 8: Trends in velocity and stride length for the X2-VelociRoACH.

the crank angle to lag in regions of the cycle which require positive torque input. Conversely, the crank angle is expected to lead in regions which require negative torque input. Fig. 9c confirms these expectations, indicating that the simulation is at least somewhat valid.

Fig. 10 shows the mechanical power the X2-VelociRoACH uses as a function of stride frequency for three different running scenarios: running on the ground, running in the air, and running in the air without legs. The mechanical power was calculated by recording electrical motor power measurements, and combining them with a model of the transmission efficiency:

$$\text{Electric power} \sim \frac{\text{Mechanical power}}{\eta} \leq \text{avg}\left(\frac{|\tau||\dot{\theta}|}{\eta}\right) \quad (1)$$

where η is the efficiency, τ is the motor torque, and $\dot{\theta}$ is the motor velocity.

The efficiency of a DC brushless motor is a direct function of its speed so we fit an efficiency model to the transmission

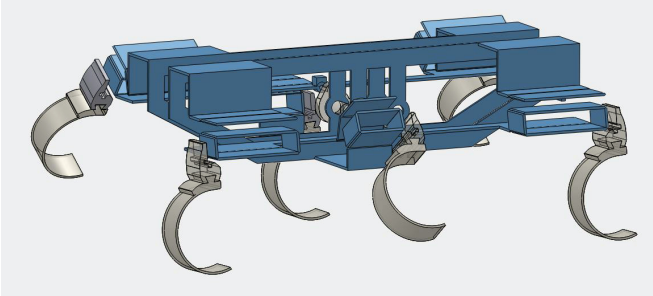

(a) A rendering of a Solidworks model of X2-VelociRoACH. The leg mechanisms have one degree of freedom, and are driven by a single virtual motor.

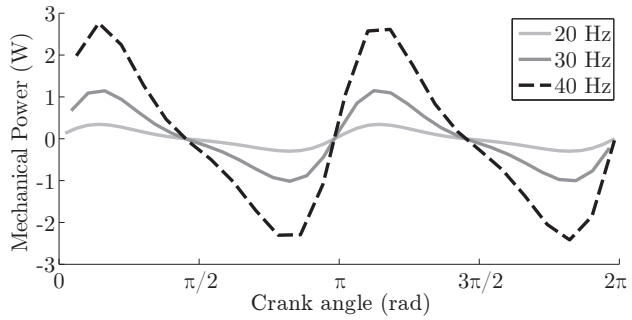

(b) Power requirements for driving the motor at constant rates, as a function of crank angle (see Fig. 4). The peak amplitude increases cubically with stride frequency.

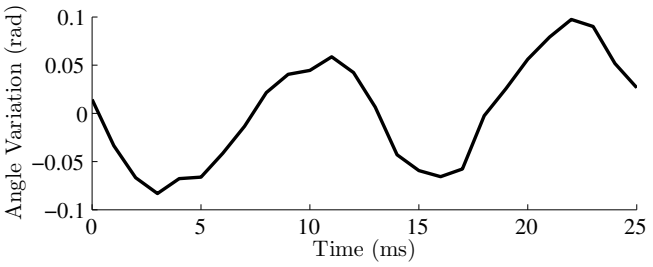

(c) Variation of crank angle over a full rotation for one in-air stride at 40 Hz, as measured by the Hall-encoder on the motor.

Fig. 9: Solidworks model of X2-VelociRoACH, used to predict power required for appendage recirculation.

by measuring the power input to the system for a range of known output loads and speeds. The efficiency of the combined brushless ESC/motor/transmission system peaked at 36%. The low-cost nature of the hobby components and the non-ideal properties of 3D printed gears make this low efficiency understandable.

Data collected from VelociRoACH [16] are shown as a point of comparison. Also shown on the graph is the predicted inertial power cost, which was calculated using the Solidworks model shown in Fig. 9a. This estimate is calculated by integrating the positive power requirements from the Solidworks model over a stride, and multiplying by the stride rate. This assumes that the sensorless ESC does no work to brake the motor, which is a safe assumption considering it lacks the transistors that would allow it to do so. This consideration is shown in the inequality in Eq. 1.

An upper bound for frictional dissipation is also shown.

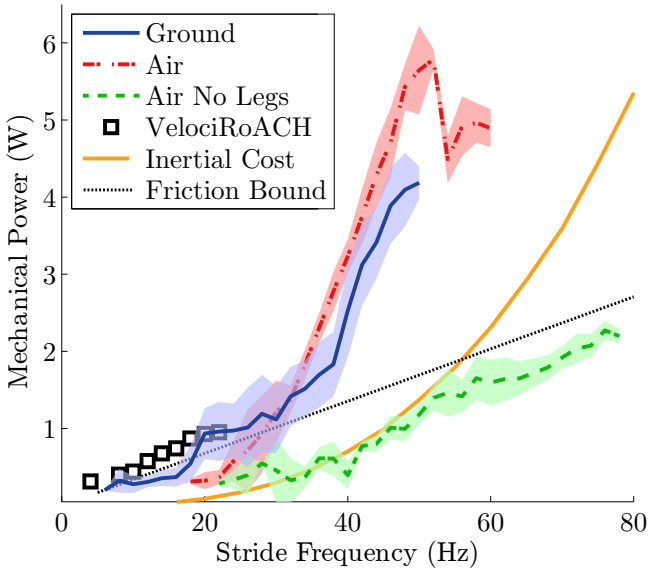

Fig. 10: Power as a function of stride frequency for the X2-VelociRoACH for running in air, with and without legs, and running on the ground. The data are segmented by individual stride; the middle line is the average, the shaded region is one standard deviation.

This upper bound is given by $P = \mu m g v_{\text{bnd}}$, where μ is the frictional coefficient (0.55), g is the gravitational constant, and v_{bnd} is the kinematic speed limit for a given frequency (from Fig. 8a). This bound corresponds to the robot being dragged along the ground at its maximum attainable speed. This is maximum amount of energy that could be dissipated by the legs using friction. When it is exceeded, we can be sure that power is being consumed by another source.

For the experimental data, the least power was consumed by the robot running in the air without its legs attached. The linear increase in this graph shows the power cost in running from only the transmission and kinematic mechanism. When the legs are added to the robot, the mechanical power requirement greatly increases. The power cost incurred by running on the ground is not greater than the power required to move the legs. There may be an issue with this data in that the order in which the trials were run may affect the trends. The robot was run in the air after it was run on the ground, so the accumulated damage may have caused the power draw in the air to be higher. In any case, the effect of running in the air vs on the ground at high frequencies is less than the effect of damage that the robot accrues during high-frequency running.

Fig. 11 shows the specific resistance of X2-VelociRoACH as a function of stride frequency. Data from VelociRoACH are provided as a reference. To allow a more direct comparison between the two platforms, the specific resistance was calculated as $S = \frac{P_m}{mgv}$ where P_m is the total *mechanical* power[6], g is the gravitational constant and v is the forward

[6]As opposed to electrical power, which is sometimes used instead

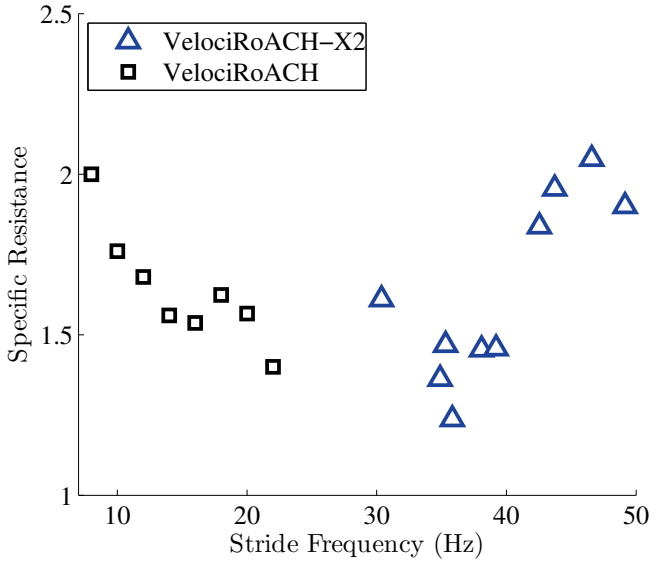

Fig. 11: Specific resistance as a function of stride frequency for the X2-VelociRoACH, and VelociRoACH [16].

velocity. The specific resistance of the X2-VelociRoACH increases at its highest speeds due to the high rates of power consumption associated with high-frequency running.

IV. Discussion

With the X2-VelociRoACH we have yet to find a fundamental speed limit for legged locomotion. The velocity increased with increased stride rate without the trend becoming sub-linear (Fig. 8a), showing that further gains in velocity can be achieved if the stride frequency can be further increased. The X2-VelociRoACH had an observed top speed of 4.9 m/s while running at 45 Hz, making it faster than the vast majority of untethered running robots in terms of absolute speed, and faster than all extant running robots in terms of relative speed (shown in Table I). One limit that was encountered was one of material strength. The loads experienced by the flexures increase with the square of the stride frequency (as predicted from Solidworks Motion simulations), so accumulated damage is especially problematic for high-frequency running. Because the gain in velocity is linear, further gains in speed (which would be accomplished by increasing stride frequency) will have diminishing returns in terms of platform survivability.

During high-frequency locomotion, the power draw of the X2-VelociRoACH is dominated by the inertial cost of recirculating the running appendages. When running above 20 Hz, the robot draws more power than the legs would be able to dissipate by any frictional interaction. We can see this inertial cost in the sharp increase in the power required for locomotion at high-speeds. When the robot is run in the air with its legs attached, it has a similar power draw to the robot running on the ground. More data collected in a properly randomized experimental trial would further elucidate these trends. The real power required to drive the legs at a constant speed (in the absence of friction) is zero, as shown by Fig. 9b. The X2-VelociRoACH has no means of storing and returning the energy fluctuations from inertial effects but if greater efficiency was desired, a flywheel or spring [4] could be added to the robot to reduce the robot's power consumption at high stride rates. This design adjustment would not mitigate the high loads applied to the flexures so a further increase in maximum speed is not expected, given the strength limits of current materials.

The large increase in power cost at high stride frequencies led to an interesting trend in the overall specific resistance of the robot. The specific resistance[7] of legged invertebrate locomotion is monotonically decreasing [12] with stride frequency. This trend is also shown in the VelociRoACH data. The fact that the specific resistance of the X2-VelociRoACH increases at its highest attainable (and furthest removed from the bio-inspired regime) stride frequencies is an important point. Locomotion at these unnaturally high frequencies is less efficient than an intermediate speed. Increasing the velocity with higher stride rates is possible, but it comes with a considerable cost in power and efficiency.

V. Conclusion

An interesting question for legged robotics is where the limits to maximal speed running come from. Most running animals prefer to run near their maximum stride frequency and increase their velocity by increasing their stride length. In this work we have shown an alternative strategy of simply increasing the stride frequency to increase velocity. This simple strategy can be readily used by biomimetic millirobots, whereas increasing stride length would require a higher degree of articulation than is available on these underactuated platforms. An alternative to a higher degree of articulation are passively extensible legs which could exaggerate the trend seen in Fig. 8b.

With the X2-VelociRoACH we have increased the stride frequency of a legged robotic platform far beyond what an animal of equivalent size would use. This platform runs at a higher stride frequency than any other extant legged robot. The top speed of 4.9 m/s was observed at 45 Hz, the highest frequency the robot could use without losing appendages. The current limitation on the maximum speed of the X2-VelociRoACH is therefore one of material strength. Due to the choice of actuation scheme the minimum speed for stable running was 2.75 m/s, which makes the X2-VelociRoACH a highly specialized runner. Position based control of the brushless motor would improve the performance of this robot at low speeds.

We investigated the energetic costs associated with high-frequency running. The power demand increases greatly at high stride frequencies due to the rapidly cycling the running appendages. This causes the specific resistance of the platform to increase at its highest attainable speeds. This trend is uncommon to animal locomotion, because animals increase stride length instead of stride frequency [13].

[7]Cost of Transport is reported in [12]. Specific resistance is cost of transport normalized by the gravitational constant.

TABLE I: COMPARISON TO SIMILAR RUNNING ROBOTS

	X2-VelociRoACH	**VelociRoACH** [16]	**DynaRoACH** [19]	**iSprawl** [22]	**Research RHex** [27]
External Dimensions (LxWxH) (cm)	10.4 x 6.4 x 4.9	10 x 6.5 x 4.2	10 x 4.5 x 3	15.5 x 11.6 x 0.7	54 x 39 x 12
Mass (g)	54.6	29.1	23.7	300	8200
Top Speed (body-lengths/second)–(m/s)	47 (4.9)	27 (2.7)	14 (1.4)	15 (2.3)	5 (2.7)
Stride Frequency (Hz)	45	24	20	14	6
Specific Resistance (Electric power)	3.3	0.98	1.1	1.75	0.72

While using stride frequencies far removed from the bio-inspired regime, the power consumption of the X2-VelociRoACH is dominated by inertial forces. The gain in velocity with stride frequency is linear, whereas the power costs increase cubically. These diminishing gains in velocity motivate other strategies for increasing the speed of the platform.

VI. FUTURE WORK

There are properties of high-frequency gaits other than energetic cost which could be studied in the future. The rapid and impactful manner in which the running appendages interact with the ground should give rise to interesting frictional interactions. To isolate experimental variables of interest only carpet was used in this work, but many more terrains could be investigated. High frequency gaits on granular terrain would also be an interesting subject of study.

Frequency based trends in running gait metrics such as duty factor or touchdown angle would be interesting to study. Unfortunately, the robot's leg motion was not sufficiently discernible in our high-speed videos to be able to study these properties rigorously.

ACKNOWLEDGMENTS

Thanks to the members of the Biomimetic Millisystems Lab for their helpful comments and discussions.

REFERENCES

[1] R. M. Alexander, "A dynamic similarity hypothesis for the gaits of quadrupedal mammals," *J. Zool.*, pp. 135–152, 1983.

[2] B. Andrews, B. Miller, J. Schmitt, and J. E. Clark, "Running over unknown rough terrain with a one-legged planar robot." *Bioinspir. Biomim.*, vol. 6, no. 2, p. 026009, Jun. 2011.

[3] S. S. Baek, F. L. Garcia Bermudez, and R. S. Fearing, "Flight control for target seeking by 13 gram ornithopter," *2011 IEEE/RSJ Int. Conf. Intell. Robot. Syst.*, pp. 2674–2681, Sep. 2011.

[4] S. S. Baek, K. Y. Ma, and R. S. Fearing, "Efficient resonant drive of flapping-wing robots," *IEEE Int. Conf. Intell. Robot. Syst.*, pp. 2854–2860, 2009.

[5] A. T. Baisch, O. Ozcan, B. Goldberg, D. Ithier, and R. J. Wood, "High speed locomotion for a quadrupedal microrobot," *Int. J. Rob. Res.*, May 2014.

[6] P. M. Birkmeyer, K. Peterson, and R. S. Fearing, "DASH : A dynamic 16g hexapedal robot," *IEEE Int. Conf. Intell. Robot. Syst.*, pp. 2683–2689, 2009.

[7] R. Blickhan and R. J. Full, "Locomotion energetics of the ghost crab," *Jnl. Exp. Biol.*, pp. 155–174, 1987.

[8] ——, "Similarity in multilegged locomotion: Bouncing like a monopode," *Jnl. Comp. Physiol. A Neuroethol. Sensory, Neural, Behav. Physiol.*, vol. 173, no. 5, pp. 509–517, 1993.

[9] C. Y. Brown, D. E. Vogtmann, and S. Bergbreiter, "Efficiency and effectiveness analysis of a new direct drive miniature quadruped robot," *IEEE/RSJ Int. Conf. Robot. Autom.*, pp. 5631–5637, 2013.

[10] A. D. Buchan, D. W. Haldane, and R. S. Fearing, "Automatic identification of dynamic piecewise affine models for a running robot," *2013 IEEE/RSJ Int. Conf. Intell. Robot. Syst.*, pp. 5600–5607, Nov. 2013.

[11] J. E. Clark, D. I. Goldman, P.-c. Lin, G. a. Lynch, T. S. Chen, H. Komsuoglu, R. J. Full, and D. E. Koditschek, "Design of a bio-inspired dynamical vertical climbing robot," *Robot. Sci. Syst.*, 2007.

[12] R. J. Full, "The Concepts of Efficiency and Economy in Land Locomotion," in *Effic. Econ. Anim. Physiol.*, R. W. Blake, Ed. Cambridge Univ Pr, 1991, pp. 97–131.

[13] ——, "Mechanics and Energetics of Terrestrial Locomotion: Bipeds to Polypeds," in *Energy Transform. Cells Org.* Verlag, 1989.

[14] R. J. Full and M. S. Tu, "Mechanics of a rapid running insect: two-, four- and six-legged locomotion." *Jnl. Exp. Biol.*, vol. 156, pp. 215–31, Mar. 1991.

[15] D. W. Haldane and R. S. Fearing, "Using dynamic similarity scaling to inspire the design of a high-speed hexapedal millirobot," in *Soc. Integr. Comp. Biol.*, 2013.

[16] D. W. Haldane, K. C. Peterson, F. L. Garcia Bermudez, and R. S. Fearing, "Animal-inspired Design and Aerodynamic Stabilization of a Hexapedal Millirobot," *IEEE/RSJ Int. Conf. Robot. Autom.*, 2013.

[17] N. C. Heglund, C. R. Taylor, and T. A. McMahon, "Scaling stride frequency and gait to animal size: mice to horses." *Science*, vol. 186, no. 4169, pp. 1112–3, Dec. 1974.

[18] K. L. Hoffman and R. J. Wood, "Passive undulatory gaits enhance walking in a myriapod millirobot," *IEEE/RSJ Int. Conf. Intell. Robot. Syst.*, vol. 2, pp. 1479–1486, 2011.

[19] A. M. Hoover, S. Burden, X. Y. Fu, S. S. Sastry, and R. S. Fearing, "Bio-inspired design and dynamic maneuverability of a minimally actuated six-legged robot," in *3rd IEEE EMBS Int. Conf. Biomed. Robot. Biomechatronics*, Sep. 2010, pp. 869–876.

[20] A. M. Hoover and R. S. Fearing, "Fast scale prototyping for folded millirobots," *IEEE Int. Conf. Robot. Autom.*, pp. 886–892, 2008.

[21] P. E. Hudson, S. a. Corr, and A. M. Wilson, "High speed galloping in the cheetah (Acinonyx jubatus) and the racing greyhound (Canis familiaris): spatio-temporal and kinetic characteristics." *J. Exp. Biol.*, vol. 215, no. Pt 14, pp. 2425–34, Jul. 2012.

[22] S. Kim, J. E. Clark, and M. R. Cutkosky, "iSprawl: Design and Tuning for High-speed Autonomous Open-loop Running," *Int. Jnl. Robot. Res.*, vol. 25, no. 9, pp. 903–912, Sep. 2006.

[23] N. J. Kohut, K. C. Peterson, D. Zarrouk, and R. S. Fearing, "Aerodynamic Steering of a 10 cm High-Speed Running Robot," *IEEE/RSJ Int. Conf. Intell. Robot. Syst.*, 2013.

[24] N. J. Kohut, A. O. Pullin, D. W. Haldane, D. Zarrouk, and R. S. Fearing, "Precise Dynamic Turning of a 10 cm Legged Robot on a Low Friction Surface Using a Tail," *IEEE Int. Conf. Robot. Autom.*, 2013.

[25] D. Lentink, S. R. Jongerius, and N. L. Bradshaw, "The Scalable Design of Flapping Micro-Air Vehicles Inspired by Insect Flight," in *Fly. Insects Robot.*, D. Floreano, J.-C. Zufferey, M. V. Srinivasan, and C. Ellington, Eds. Berlin, Heidelberg: Springer-Verlag Berlin Heidelberg, 2010, pp. 185–205.

[26] A. Pullin, N. J. Kohut, D. Zarrouk, and R. S. Fearing, "Dynamic turning of 13 cm robot comparing tail and differential drive," *IEEE Int. Conf. Robot. Autom.*, pp. 5086–5093, 2012.

[27] J. D. Weingarten, G. A. D. Lopes, M. Buehler, R. E. Groff, and D. E. Koditschek, "Automated Gait Adaptation for Legged Robots," *IEEE Int. Conf. Robot. Autom.*, 2004.